Applied Radiation and Isotopes 182 (2022) 110126

Contents lists available at ScienceDirect

Applied Radiation and Isotopes

journal homepage: www.elsevier.com/locate/apradiso

Identification of ESR centers and their role in the TL of natural salt from Lluta, Peru

Darwin J. Callo-Escobar [a,**], Nilo F. Cano [b,*], T.K. Gundu Rao [a], Carlos D. Gonzales-Lorenzo [a], Klinton V. Turpo-Huahuasoncco [a], Yolanda Pacompia [a], Monise B. Gomes [c], Jose F. Benavente [d], Jose F.D. Chubaci [c], Shigueo Watanabe [c], Jorge S. Ayala-Arenas [a]

[a] Escuela Profesional de Física, Facultad de Ciencias Naturales y Formales, Universidad Nacional de San Agustín de Arequipa (UNSA), Av. Independencia S/N, Arequipa, Peru
[b] Instituto do Mar, Universidade Federal de São Paulo, Rua. Doutor Carvalho de Mendonça, 144, CEP, 11070-100, Santos, SP, Brazil
[c] Instituto de Física, Universidade de São Paulo, Rua do Matão, Travessa R, 187, CEP, 05508-090, São Paulo, SP, Brazil
[d] CIEMAT, Av. Complutense 40, E, 28040, Madrid, Spain

ARTICLE INFO

Keywords:
NaCl
Defects centers
Radiation effects
ESR
TL

ABSTRACT

In this study, the thermoluminescence (TL) properties of natural NaCl from Lluta, Arequipa-Peru was investigated. The number of peaks and the kinetic parameters associated with the TL glow peaks of NaCl sample after gamma-irradiation were analyzed by initial rise and deconvolution method. Defect centers induced in pure salt by gamma irradiation have been studied by electron spin resonance (ESR) with a view to identify the centers associated with the TL process in the salt. Thermal annealing experiments indicate the presence of three defect centers. Center I characterized by the *g*-value 2.011 is identified as an O^- ion and relates with the dominant TL peak at 220 °C. Center II with a *g*-value of 2.0058 is attributed to a F center and is found to correlate with the 128 °C TL peak. Center III has of *g*-value 2.014 and is also assigned to an O^- ion.

1. Introduction

A considerable number of pure and doped natural and synthetic crystals produced by different synthesis techniques exhibit thermoluminescence (TL) properties. Natural crystals of well-determined TL glow peaks are promising candidates for applications in radiation dosimetry. Among the readily available natural crystals is sodium chloride (NaCl). Depending on its origin, some natural crystals have good TL properties and can therefore be used as a radiation dosimeter.

The TL properties of natural sodium chloride from different sources were investigated by different researchers (Khazal and Abul-Hail, 2010; Spooner et al., 2011, 2012; Rodriguez-Lazcano et al., 2012; Datz et al., 2016; Abdel-Wahed et al., 2016; Mehrabi et al., 2017; Ademola, 2017; Roman-Lopez et al., 2018; Wahib et al., 2020). Recently, the kinetic characterization of thermoluminescence of NaCl has been studied in different regions in the world (Druzhyna et al., 2016; Elashmawy, 2018; Azim et al., 2020; Khamis and Arafah, 2021; Ahmad et al., 2021). In NaCl collected from Khewra salt mines in Pakistan, Ahmad et al. (2021) have stated that the glow curve has two peaks around 115–130 °C and 150–170 °C, and an intense TL peak centered around 220–240 °C, which has been used for radiation dosimetry, due to its high sensitivity to gamma radiation in the range of 5 mGy–100 mGy. The same authors determined the activation energy, frequency factor and kinetic order values for the TL peaks of salt granules by the CGCD method.

Many dosimetric characteristics of TL materials mainly depend on kinetic parameters quantitatively describing the trapping-emitting centers responsible for the TL emission. Thus, the determination of the kinetic parameters is an active area of research. There are various methods for evaluating the trapping parameters from TL glow curves (Chen and McKeever, 1997; McKeever, 1985), which may be broadly classified as methods applied to single or highly isolated glow peaks, and methods applied to complex glow curves. Some methods as the initial rise, variable heating rates and peak shape are suitable for the single or highly isolated glow peaks. Thermal annealing and computerized glow curve deconvolution are methods suitable for the complex glow curves. The first is to isolate each individual TL peak from the others using

* Corresponding author.
** Corresponding author.
E-mail addresses: dcallo@unsa.edu.pe (D.J. Callo-Escobar), nilocano@if.usp.br, nilo.cano@unifesp.br (N.F. Cano).

https://doi.org/10.1016/j.apradiso.2022.110126
Received 8 November 2021; Received in revised form 22 January 2022; Accepted 23 January 2022
Available online 25 January 2022

partial thermal annealing treatment (Borbón-Nuñez et al., 2014) and the other is to make a complete glow curve analysis using deconvolution (Kitis et al., 1998; Benavente et al., 2019).

The aims of many studies are to investigate the possibility of employing these crystals for dosimetry purposes or to understand the trap structure and defects in the materials.

The defect centers created by ionizing radiation are responsible for TL emission. The identification and characterization of irradiation-induced defects in these materials is necessary to elucidate the charge transfer mechanisms during the TL phenomenon. The complete information concerning the charge traps in the TL mechanism cannot be acquired by carrying TL measurements alone. In this context, there is ESR technique, which can be helpful to find more information about paramagnetic species such as charge traps (trapped hole or an electron). In general, the ESR technique provides a non-destructive way to obtain information about possible centers responsible for TL emission through correlation studies between TL and ESR techniques.

The physical basis of the TL signal in the NaCl crystal has been discussed by some authors in the framework of the role of color centers, especially the F-center. Gartia (2009) has studied the feasibility of thermal annealing of F-centers correlated to all TL peaks in the TL glow curve of NaCl. However, there is no record of a correlation study between TL and ESR to identify the centers responsible for TL light emission in natural salt samples.

The objective of this work is focused on the identification of the point defects responsible for the TL emission of Lluta natural salt from Arequipa, Peru. Further, the study aims to determine the kinetic parameters associated with the TL peaks, such as activation energy, frequency factor and kinetic order of each peak at room temperature.

2. Experimental details

The natural salt sample investigated in this work was collected at the Lluta mine, Arequipa, Peru. This mine is located at the intersection of the following geographic coordinates: latitude 15°58′45.75″ S and longitude 71°59′24.84″ W.

The salt sample from Lluta (SLL) was cleaned and then crushed using a mortar and turned into a fine powder of grain size between 75 and 150 μm for TL and ESR measurements, while grains smaller than 75 μm in diameter were used in structural analysis and chemical composition by X-ray diffraction (XRD) and X-ray fluorescence (XRF) methods, respectively. Before any TL or ESR measurements, the SLL samples were heat treated at a temperature of 500 °C for 30 min to remove any signal due to energy absorption from their geological formation.

X-ray diffraction (XRD) was carried out by means of a Rigaku model MiniFlex 600 X-ray diffractometer equipped using 40 kV voltages and 15 mA current with Cu K_α-radiation, to study the structural characteristics of the pure salt sample. The measurements were made in an angular range of 2θ from 20 to 80° with 0.02° step size and a scan rate of 0.6 s. The sample was crushed into fine powder prior to XRD measurement and was performed at room temperature. An X-ray fluorescence (XRF) spectrometer Malvern PANalytical, model Zetium of the Laboratory of Technological Characterization from the Polytechnic School of the University of São Paulo was used to analyze the elemental composition of the SLL sample.

TL glow curves were recorded 24 h after irradiation on a TL reader having an EMI 9235QB photomultiplier tube (PMT) through a combination of a BG3 and a BG39 filter (overall transmission band 350–450 nm). The glow curve was recorded between 50 and 300 °C with a heating rate of about 4 °C/s in a flow of an inert nitrogen gas. For each TL measurement, a constant weight of 4 mg of powdered sample with grain size between 75 and 150 μm was taken. Five TL reading measurements were carried out to obtain an average TL glow curve.

ESR measurements were carried out using a Freiberg Instruments MiniScope ESR spectrometer Model 5500 at room temperature and operating at the X-band frequency with the following instrument parameters: sweep time: 120 s, modulation amplitude: 0.2 mT, modulation frequency: 100 kHz, microwave power: 20 mW. The SLL samples were irradiated at 10 kGy gamma dose before recording their ESR spectra. ESR intensity was measured by peak-to-peak amplitude. Diphenyl Picryl Hydrazyl (DPPH) was used to calibrate the *g*-factors of defect centers.

For TL measurements, SLL samples were irradiated with different gamma radiation doses, ranging from 10 Gy up to 1 kGy, using a ^{60}Co source with a dose rate of 442.97 Gy/h.

3. Results and discussion

X-ray diffraction studies are used to reveal the nature of the crystallinity of the as-received (SLL-AR) sample and the sample heat-treated at 500 °C (SLL-TT500). The powder XRD patterns of both samples (SLL-AR and SLL-TT500) are shown in Fig. 1. They are in a good agreement with the NaCl reference pattern and clearly confirm the purity of their crystalline phase. Rietveld refinement analysis of the XRD pattern indicates the presence of the halite crystalline phase and a small concentration of anhydrite. From this fact, the XRD patterns have been fitted with a monoclinic unit cell and to the Fm-3m space group.

Table 1 shows the composition in weight % of the elements of the SLL sample using the XRF analysis; several elements were not listed (with less than 0.01%) in the table and some elements were not detected due to limitations of the XRF technique. This analysis was performed to identify the chemical elements in the samples and for future studies about which of these elements are responsible for the TL and ESR signals. Besides basic components Na and Cl, elements such as Ca, S, Si, and others in smaller concentrations are found.

TL glow curves of SLL-TT500 samples were measured from room temperature to 300 °C after irradiating the samples at different doses of Co-60 gamma radiation from 10 Gy to ~1 kGy. It is well demonstrated that the glow curve structures are of specific significance as they are the main indicators of whether or not a material can be employed for TL dosimetry. The favorable glow curve structure, luminescence efficiency and TL sensitivity are strongly influenced by the concentration of points

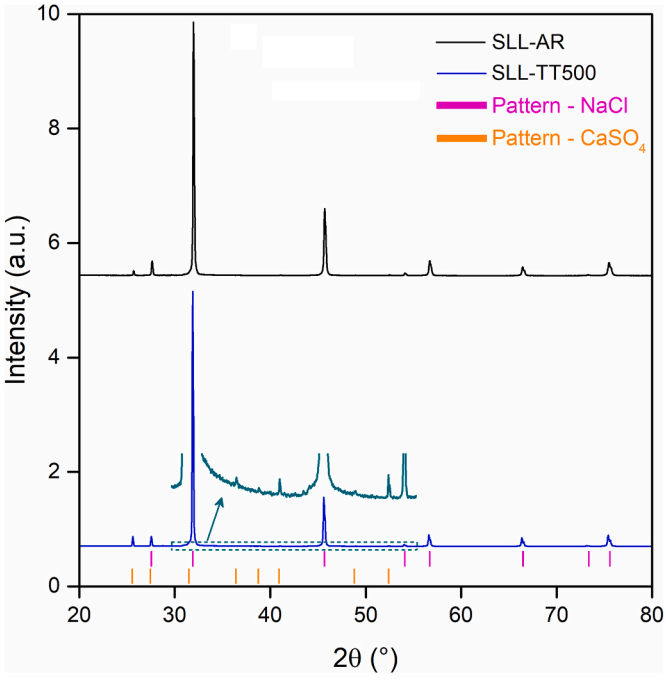

Fig. 1. X-ray diffraction of the salt sample from Lluta: sample as-received (top - black line) and the sample with thermal pretreatment at 500 °C for 30 min (bottom - blue line). (For interpretation of the references to color in this figure legend, the reader is referred to the Web version of this article.)

Table 1
Elemental composition by X-ray fluorescence (XRF) analysis of the natural salt sample from Lluta.

Sample	Elements (%)												
Salt	Cl	Na	Ca	S	Si	Mg	Al	Fe	K	As	P	Br	Sr
	60.0	35.7	2.83	0.93	0.21	0.09	0.09	0.04	0.03	0.02	<0.01[a]	<0.01[a]	<0.01[a]

[a] 0.01% - limit of quantification by the XRF method used.

defects in the material. The concentration of these defects plays a very important role during the thermoluminescence phenomenon. These defects can act as trapping or recombination centers in the thermoluminescent material. The identification of these defects or TL centers is possible through spectroscopic techniques, such as ESR.

The TL glow curve response as a function of temperature is shown in Fig. 2. The TL glow curve of SLL-TT500 sample consists of four peaks, one at 220 °C and another of small intensity at 120, 160 and 270 °C. These glow curves are similar with those reported by Ahmad et at. (2021). The glow peak position and the shape of the glow curve remained unchanged at all doses and only variation in TL intensity was observed. The TL peak intensities were observed to increase with increasing gamma dose. In the inset of Fig. 2, the dose response of the main peak at 220 °C shows a linear behavior from 10 Gy to 100 Gy, and later saturates.

Most minerals of the Earth's upper mantle have minor amounts of hydroxyl (OH) groups. The OH concentration in each mineral species is variable and dependent on the geological setting and mineral formation. In the published literature, it is reported that most of the geological minerals exhibit non-radiation induced spurious thermoluminescence (Bell and Rossman, 1992; Douglas and Budd, 1981; Pagonis et al., 1997) from the surface of the phosphor grains, while TL emitted from gamma irradiated phosphor grains is a volume effect. Intensity of spurious TL can be reduced by making TL measurements in pure nitrogen or argon atmosphere. None of the well-known TLD phosphors like $CaSO_4$:Dy, CaF_2:Dy, LiF:Mg,Ti, LiF:Mg,Cu,P, Al_2O_3:C etc. are prone to this effect. In the present study all TL measurements were taken with flow of inert nitrogen gas using phosphor grains in the range 75–150 μm. Thus, due to combined effect of forementioned parameters it is difficult to discern contribution of surface traps from the composite TL glow curve of phosphor grains for gamma dose of ≥1 Gy-typical dose used for study TL phosphors.

The activation energies of the SLL-TT500 sample were determined experimentally using the initial rise method in combination with the E-T_{STOP} method. This method allows the identification of TL peaks overlapping each other in the TL glow curve, which are normally difficult to identify. In this method, initially a sample amount of SLL-TT500 is irradiated with 10 Gy. Then, an aliquot of this sample was heated from room temperature up to temperature of stop (T_{STOP}), and allowed to cool naturally to room temperature, and later the TL glow curve measurement is carried out. We repeated the procedure for different T_{STOP} values, i.e., the cycle of heating, cooling and reading the TL curve for each T_{STOP} in 5 °C steps from 55 °C to 280 °C was performed. The TL glow curves obtained with this method were used to determine the activation energy of the individual peaks by using the initial rise method for each T_{STOP}. If we plot the curve, activation energy function T_{STOP} values (i.e., E-T_{STOP} curve), the resulting curves look like staircases shaped, and each plateau region indicates the activation energy of an individual TL peak. Fig. 3 shows the graph of the activation energy versus T_{STOP} of the previously presented method. Different trapping levels thus obtained by this method are shown in Fig. 3. The activation energies indicate shallow traps as well as deeper traps within the SLL-TT500 sample. From the analysis of the glow curve and the E-T_{STOP} graph we can conclude that the main trapping levels play an important role in radiation storage.

As seen in Fig. 2, the TL glow curve of SLL-TT500 sample possibly contains several peaks superimposed on each other. In addition, this figure shows a negligible shift in the position of the TL peak maxima with increase in dose and this result indicates that the charge transfer processes are associated with first-order kinetics. Therefore, for the deconvolution of the TL emission curve of the SLL-TT500 sample we use

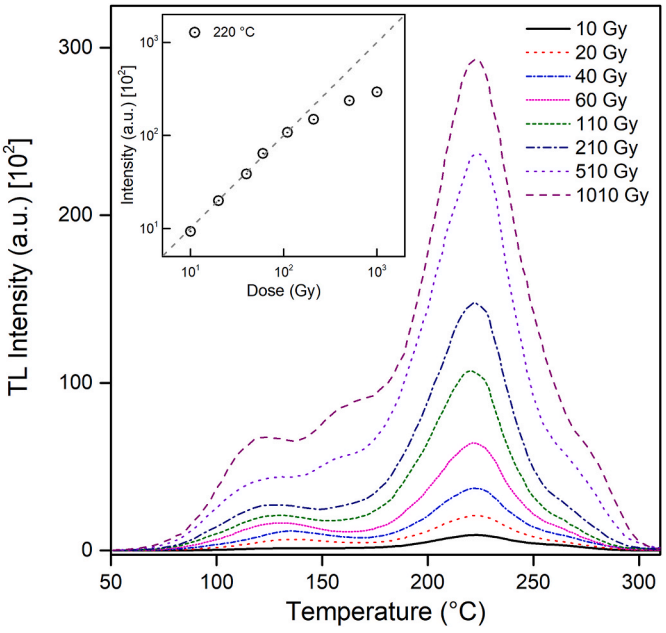

Fig. 2. TL glow curves of salt from Lluta previously annealed at 500 °C/30min and irradiated with different doses of gamma radiation. In the inset, behavior of the TL intensity of the 220 °C peak as a function of gamma radiation doses, the dashed line indicates linearity.

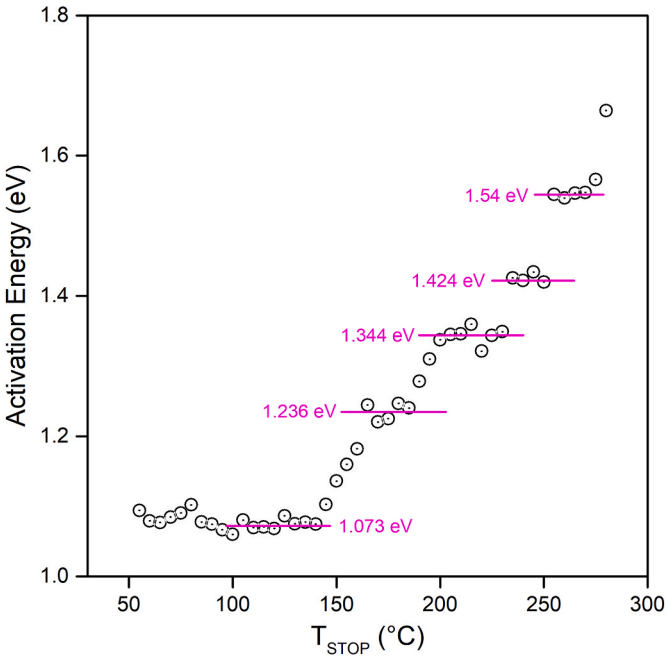

Fig. 3. Activation energy vs. T_{STOP} obtained by the initial rise method.

a linear combination of functions related to first order kinetics (FOK) with continuous trap distributions (Benavente et al., 2019).

Fig. 4 represents the deconvoluted graph for the SLL sample annealed at 500 °C and irradiated with a gamma dose of 1010 Gy using a linear combination of five functions related to the FOK approach with continuous contributions of traps related to a Gauus distribution (inset of Fig. 4). This result shows the presence of the same five TL peaks obtained by E-T_{STOP} method. Table 2 shows the different trapping parameters such as: maximum temperature, activation energy, distribution width and frequency factor calculated by deconvolution method for two samples irradiated with 10 Gy and 1010 Gy. Figure of merit (FOM) (Balian and Eddy, 1977; Afouxenidis et al., 2012) of the theoretical fit to the experimental data is only 1.14% for sample irradiated with 1010 Gy, which indicates the good agreement between the theoretical and experimental data. When we compare the experimental results from E-T_{STOP} analysis and the theoretical fitted parameters from deconvolution method, both results show a good correlation with each other.

The room temperature electron spin resonance (ESR) spectrum of gamma irradiated pure natural salt (SLL-TT500) is displayed in Fig. 5. The SLL-TT500 sample was irradiated with a gamma dose of 10 kGy. It was inferred from thermal annealing and dose response experiments that three defect centers contribute to the observed spectrum. These centers are labeled in Fig. 5. Center I is characterized by a *g*-value equal to 2.011 and a linewidth of 7 G.

NaCl crystallizes in the cubic Fm-3m space group (Kittel, 1976). The structure is composed of Na^+ ions bonded to six equivalent Cl^- ions. Na^+ ions occupy all octahedral sites. Each chloride ion is also surrounded by six sodium ions which are located at the corners of a regular octahedron. Therefore, the cations and anions are present in equivalent positions. Each atom is symmetrically surrounded by six chlorine atoms and vice versa.

Center I is characterized by an isotropic *g*-value equal to 2.011 and a linewidth of 7 G. The line is slightly broad and indicates a possible unresolved hyperfine structure. Nuclear spins in proximity can interact with the unpaired electron resulting in unresolved hyperfine structure.

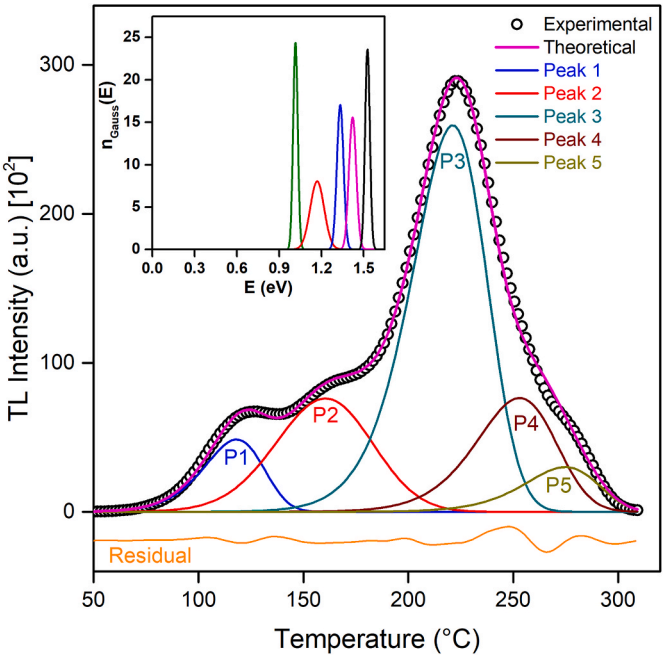

Fig. 4. Deconvoluted glow curves of Lluta mines salt sample for dose of 1010 Gy. A good fit between the experimental glow curve (black circles) and the theoretical glow curve (pink line) was obtained assuming the presence of five peaks. In the inset, the Gaussian distribution used for the deconvolution of each TL peak. (For interpretation of the references to color in this figure legend, the reader is referred to the Web version of this article.)

Table 2
Details of maximum temperature (T_M), activation energy (*E*), distribution width (σ), frequency factors (*s*) for each deconvolved peak in the glow curve.

Dose	Peak	T_M (°C)	*E* (eV)	σ (eV)	*s* (s^{-1})
10 Gy	P1	122	1.01	0.0180	$2.3{\cdot}10^{12}$
	P2	164	1.16	0.0518	$7.7{\cdot}10^{13}$
	P3	221	1.35	0.0236	$1.7{\cdot}10^{13}$
	P4	253	1.44	0.0211	$1.4{\cdot}10^{13}$
	P5	265	1.57	0.0163	$1.3{\cdot}10^{14}$
1010 Gy	P1	119	1.02	0.0164	$3.4{\cdot}10^{12}$
	P2	165	1.17	0.0496	$7.9{\cdot}10^{13}$
	P3	223	1.33	0.0234	$8.8{\cdot}10^{13}$
	P4	255	1.42	0.0256	$8.7{\cdot}10^{13}$
	P5	276	1.53	0.0169	$2.5{\cdot}10^{13}$

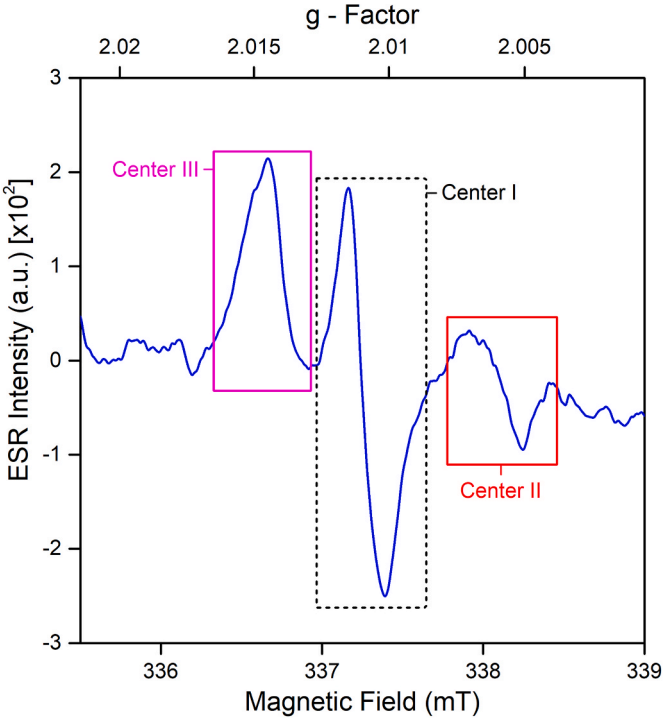

Fig. 5. Room temperature ESR spectrum of irradiated pure salt (gamma dose: 10 kGy). Line labeled as center I is due to an O^- ion. Center II line is assigned to a F center and center III is also attributed to an O^- ion.

Na^+ and Cl^- in NaCl have isotopes with nuclear spins 3/2 viz., ^{23}Na, ^{35}Cl and ^{37}Cl. ^{23}Na has a natural abundance of 100%, while ^{35}Cl and ^{37}Cl have 75.8% and 24.2% abundance respectively (Weast, 1971). The nuclear magnetic moment of ^{23}Na (2.22) is much higher than ^{35}Cl (0.822) and ^{37}Cl (0.684). The electronic spin can therefore interact with ^{23}Na as well as ^{35}Cl and ^{37}Cl. Due to the presence of impurities and non-stoichiometry, defect centers can be created in NaCl. F centers can be formed in the presence of anion vacancies in the lattice. On the other hand, Na^+ vacancies can trap holes leading to the formation of V-centers (Holston et al., 2015). The slightly large linewidth of center I indicates possible interaction with nearby nuclei. Therefore, center I is tentatively assigned to an O^- ion.

Känzig and Cohen (1959) have examined in detail a paramagnetic center observed in several alkali halides (chlorides, bromides and iodides of sodium, potassium and rubidium). They considered the diatomic molecule ion O_2^- as the most probable defect center in these alkali halides. Absence of hyperfine splitting and the relatively large g-shift displayed by the center indicated that the defect center could be O_2^- ion. For example, in KCl, the observed principal *g*-values were $g_1 = 2.4359$, $g_2 = 1.9512$, and $g_3 = 1.9551$. Strong support for this

assignment came from the observation that the concentration of the defect center was greatly enhanced by heating the crystal in an oxygen atmosphere. On the other hand, heating the crystal in other environments like vacuum and hydrogen greatly reduced the concentration to undetectable amounts.

Considering that O_2^- ion is generally observed in alkali halides, as pointed out by Känzig and Cohen (1959), it may not be unusual that O^- ion can be observed in NaCl lattice. The defect center O_2^- in alkali halides (Känzig and Cohen, 1959) is derived from O_2^{2-} molecule ion located in the space left by a missing anion. It is speculated that the center I (O^- ion) observed in the present study is derived from O_2^{2-} ion or O^{2-} ion present in the NaCl lattice. Fig. 6 shows a model of O^- ion in the present NaCl lattice.

In the spinel $MgAl_2O_4$, a center with features similar to center I has been observed (Ibarra et al., 1991). An ESR signal with a *g*-value 2.011 is found due to X-irradiation and displays an optical absorption band at about 3.4 eV. The authors conclude that the center responsible for the absorption band and the associated ESR signal is a hole trapped cation vacancy i.e., a V-type center formed by hole trapping at oxygen ions surrounding cation vacancies. The unpaired spin occupies an oxygen *p*-orbital in an O^- ion. A cation vacancy close to O^- ion provides stability to the hole on the oxygen ion due to electrostatic attraction. A positive *g*-shift results from a hole trapped in an oxygen p_z-orbital. The observed *g*-value of center I is in accordance with this expectation.

A pulsed thermal annealing method was used to measure the stability of center I. The sample was heated to a specific temperature and was maintained at that temperature for 3 min. ESR experiments were carried out after cooling the sample to room temperature. The results of these experiments are shown in Fig. 7. It is seen that the center becomes unstable at about 170 °C and decays in the temperature range 170 °C–270 °C. This decay indicates that center I may correlate with the 220 °C TL peak in SLL sample.

Center II (Fig. 5) has a g-value equal to 2.0058 and a linewidth of 6.4 G. Anion vacancies present in the system due to reasons mentioned earlier and also by their creation by gamma irradiation can trap electrons forming F centers. One of the earlier systems in which F center was studied by ESR is LiF (Hutchison, 1949). In this system, the center was characterized by a *g*-value close to free-spin value (2.0023) and a linewidth that was surprisingly large (~100 G). However, it may be mentioned that the inherent linewidth of a F center is quite small and is about 1 G as observed in MgO (Wertz et al., 1957). The natural

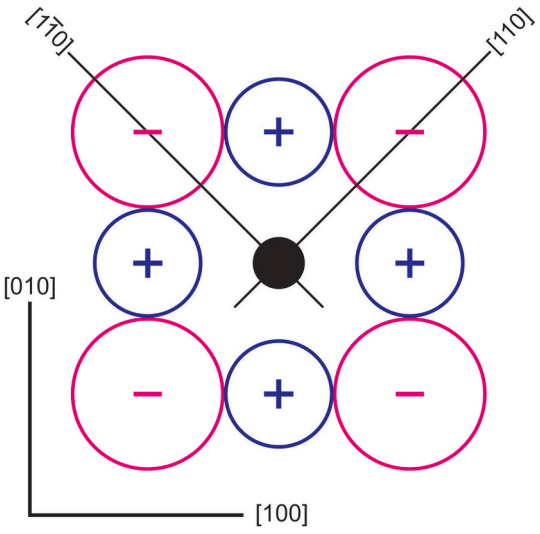

Fig. 6. Model of O^- center in NaCl lattice as derived from Känzig and Cohen (1959). Pink circle is Cl^- ion, blue circle is Na^+ ion and black circle is O^- ion. (For interpretation of the references to color in this figure legend, the reader is referred to the Web version of this article.)

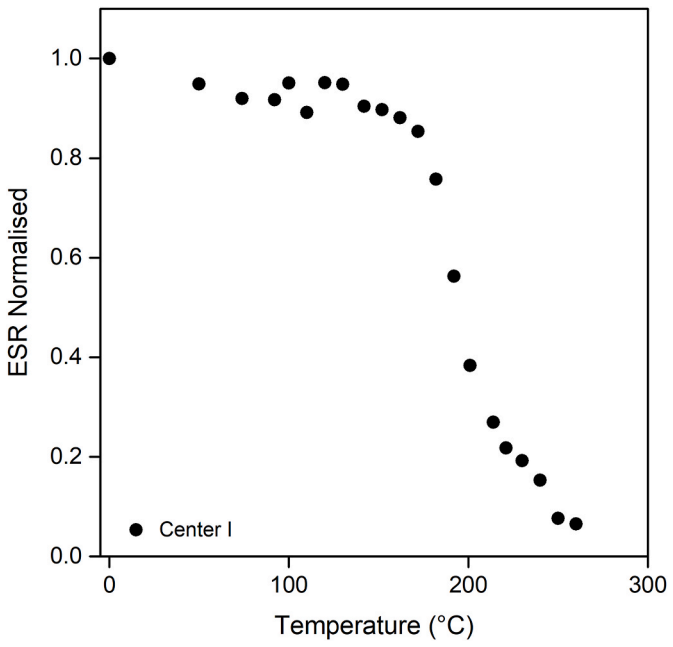

Fig. 7. Thermal annealing behavior of center I in the salt sample.

abundance of the isotopes of ions in a compound and the magnitude of magnetic moments decide the linewidth. In alkali halide systems, large linewidths are seen as there is considerable delocalization of the electron and an interaction with multiple alkali and halide ions from successive neighboring shells. In systems like KCl and LiCl (Holton and Blum, 1962), large linewidths are observed viz., 20 G and 58 G respectively. On the other hand, F center in BaO (Tench and Nelson, 1967) displays a small linewidth of 3.5 G. Apart from alkali halides, F center has also been observed in oxide systems (an electron trapped at oxygen ion vacancy). The main feature of F center in all these systems is a *g*-value that is close to free-spin value (2.0023) and a *g*-shift which may be positive or negative. An example of a study where F center has been observed recently is in pure and defective TiO_2 nanoparticles (Choudhury and Choudhury, 2014). In the present pure salt system, *g*-shift is small and the linewidth is not large. On the basis of these observations, center II is assigned to a F center.

Fig. 8 shows the thermal annealing behavior of center II. It is seen that the intensity of the ESR signal decreases in the temperature range from about 100 °C to 230 °C. Therefore, center II could be associated with the TL peak at 128 °C.

Center III (Fig. 5) is characterized by a *g*-value equal to 2.0014 and linewidth of 7 G. Based on the reasons mentioned earlier for center I, center III is also ascribed to O^- ion. The thermal annealing behavior of the center is shown in Fig. 9. It is observed that there is scatter in the intensity of the line throughout the annealing temperature range. This makes it difficult to correlate this center with the observed TL peaks in pure salt system and no specific TL role could be assigned to this center.

4. Conclusions

The XRD, XRF, TL and ESR spectra have been measured for the salt of natural NaCl from Lluta, Arequipa-Peru. XRD pattern of the natural salt sample with or without heat pretreatment revealed the presence of two crystalline phases, being predominant the phase due to Hyalite, and a lower percentage phase due to anhydrite. Samples irradiated with gamma dose show four TL peaks, a main intense peak at 220 °C and three low intensity peaks at 120, 160 and 270 °C. The TL intensity as a function of dose in the logarithmic representation of the main peak at 220 °C shows that the peak grows linearly between 10 and 100 Gy, and then saturates. Initial rise method and deconvolution analysis showed

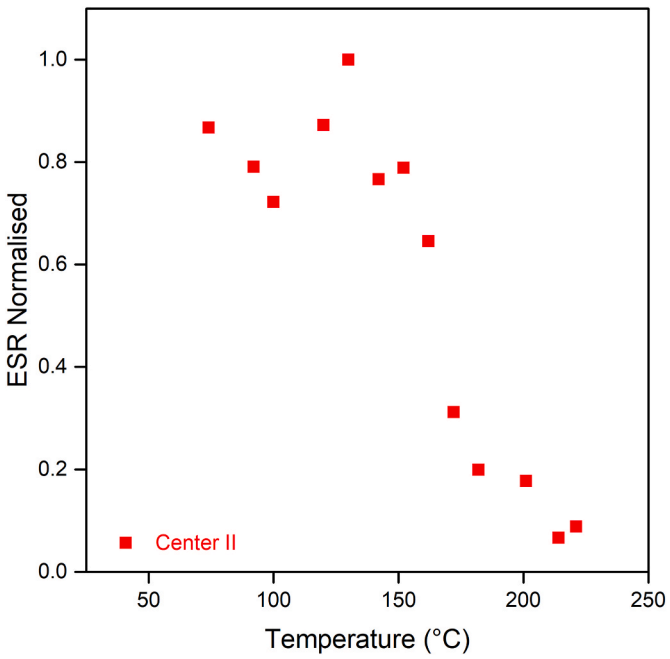

Fig. 8. Thermal annealing behavior of center II in the salt sample.

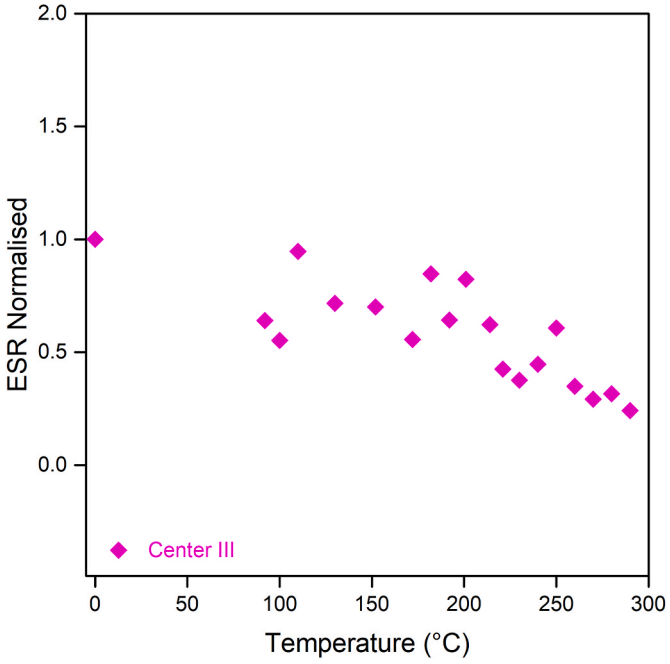

Fig. 9. Thermal annealing behavior of center III in the salt sample.

the presence of five TL glow peaks. Three defect centers have been identified in the salt system. These centers are assigned to O^- ions and a F center. O^- ion (center I) correlates with the dominant TL peak at 220 °C. F center (center II) relates to the 128 °C peak while center III is not associated with any of the observed TL peaks in pure salt.

CRediT authorship contribution statement

Darwin J. Callo-Escobar: Investigation, Conceptualization, Methodology. **Nilo F. Cano:** Writing – original draft, Supervision, Funding acquisition, Conceptualization, Project administration, Writing – review & editing. **T.K. Gundu Rao:** Writing – original draft, Validation, Investigation, Visualization. **Carlos D. Gonzales-Lorenzo:** Methodology, Validation. **Klinton V. Turpo-Huahuasoncco:** Investigation. **Yolanda Pacompia:** Investigation. **Monise B. Gomes:** Investigation, Methodology. **Jose F. Benavente:** Methodology, Validation. **Jose F.D. Chubaci:** Investigation. **Shigueo Watanabe:** Resources, Supervision. **Jorge S. Ayala-Arenas:** Funding acquisition, Supervision.

Declaration of competing interest

The authors declare that they have no known competing financial interests or personal relationships that could have appeared to influence the work reported in this paper.

Acknowledgements

The authors would like to express thanks to Ms. E. Somessari from the Institute for Energy and Nuclear Researches (IPEN), Brazil, for kindly carrying out the gamma irradiation of the samples. This work was carried out with financial support from UNSA-Investiga, Peru (Process number IBAIB-02-2018-UNSA). The authors are greatly indebted to Dr. B.C. Bhatt, ex Bhabha Atomic Research Center, Trombay, Mumbai, India.

References

Abdel-Wahed, M.H., Abdou, S.M., Abdel-Ghany, H., Amer, H.A., 2016. Thermoluminescence characteristics of NaCl from different origins. J. Sci. Res. Sci. 33, 201–213. https://doi.org/10.21608/JSRS.2016.15553.

Ademola, J.A., 2017. Luminescence properties of common salt (NaCl) available in Nigeria for use as accident dosimeter in radiological emergency situation. J. Radiat. Res. Appl. Sci. 10, 117–121. https://doi.org/10.1016/j.jrras.2017.01.003.

Afouxenidis, D., Polymeris, G.S., Tsirliganis, N.C., Kitis, G., 2012. Computerised curve deconvolution of TL/OSL curves using a popular spreadsheet program. Radiat. Protect. Dosim. 149, 363–370. https://doi.org/10.1093/rpd/ncr315.

Ahmad, K., Kakakhel, M.B., Hayat, S., Wazir-ud-Din, M., Mahmood, M.M., Rehman, S.U., Siddique, M.T., Mirza, S.M., 2021. Thermoluminescence study of pellets prepared using NaCl from Khewra salt mines in Pakistan, radiat. Environ. Bioph. 60, 365–375. https://doi.org/10.1007/s00411-021-00894-x.

Azim, M.K.M., Sani, S.F.A., Daar, E., Khandaker, M.U., Almugren, K.S., Alkallas, F.H., Bradley, D.A., 2020. Luminescence properties of natural dead sea salt pellet dosimetry upon thermal stimulation. Radiat. Phys. Chem. 176, 108964. https://doi.org/10.1016/j.radphyschem.2020.108964.

Balian, H.G., Eddy, N.W., 1977. Figure of merit (FOM), an improved criterion over the normalized chi-squared test for assessing goodness of fit of gamma-ray spectral peaks. Nucl. Instrum. Methods 145, 389–395. https://doi.org/10.1016/0029-554X(77)90437-2.

Bell, D.R., Rossman, G.R., 1992. Water in Earth's mantle: the role of nominally anhydrous minerals. Science 255, 1391–1397. https://doi.org/10.1126/science.255.5050.1391.

Benavente, J.F., Gómez-Ros, J.M., Romero, A.M., 2019. Thermoluminescence glow curve deconvolution for discrete and continuous trap distributions. Appl. Radiat. Isot. 153, 108843. https://doi.org/10.1016/j.apradiso.2019.108843.

Borbón-Nuñez, H.A., Cruz-Vázquez, C., Bernal, R., Kitis, G., Furetta, G., Castaño, V.M., 2014. Thermoluminescence properties of sintered ZnO. Opt. Mater. 37, 398–403. https://doi.org/10.1016/j.optmat.2014.06.034.

Chen, R., McKeever, S.W.S., 1997. Theory of Thermoluminescence and Related Phenomena. World Scientific, Singapore.

Choudhury, B., Choudhury, A., 2014. Contribution of paramagnetic surface F^+ and Ti^{3+} centers to ferromagnetism in pure and defective TiO_2 nanoparticles. Sci. Adv. Mater. 6, 2115–2123. https://doi.org/10.1166/sam.2014.1969.

Datz, H., Druzhyna, S., Oster, L., Orion, I., Horowitz, Y., 2016. Study of the suitability of Israeli household salt for retrospective dosimetry. Radiat. Protect. Dosim. 170, 407–411. https://doi.org/10.1093/rpd/ncv517.

Douglas, J.A., Budd, T., 1981. Spurious TLD readings due to static electricity. Phys. Med. Biol. 26, 171–173. https://doi.org/10.1088/0031-9155/26/1/018.

Druzhyna, S., Datz, H., Horowitz, Y.S., Oster, L., Orion, I., 2016. Thermoluminescence characteristics of Israeli household salts for retrospective dosimetry in radiological events. Nucl. Instrum. Methods B 377, 67–76. https://doi.org/10.1016/j.nimb.2016.04.024.

Elashmawy, M., 2018. Study of constraints in using household NaCl salt for retrospective dosimetry. Nucl. Instrum. Methods B 423, 49–61. https://doi.org/10.1016/j.nimb.2018.03.016.

Gartia, R.K., 2009. Paleothermometry of NaCl as evidenced from thermoluminescence data. Nucl. Instrum. Methods B 267, 2903–2907. https://doi.org/10.1016/j.nimb.2009.06.106.

Holston, M.S., McClory, J.W., Giles, N.C., Halliburton, L.E., 2015. Radiation-induced defects in $LiAlO_2$ crystals: holes trapped by lithium vacancies and their role in

thermoluminescence. J. Lumin. 160, 43–49. https://doi.org/10.1016/j.jlumin.2014.11.018.
Holton, W.C., Blum, H., 1962. Paramagnetic resonance of F centers in alkali halide. Phys. Rev. 125, 89–103. https://doi.org/10.1103/PhysRev.125.89.
Hutchison, C.A., 1949. Paramagnetic resonance absorption in crystals colored by irradiation. Phys. Rev. 75, 1769–1770. https://doi.org/10.1103/PhysRev.75.1769.2.
Ibarra, A., Lopez, F.J., Castro, J., 1991. V centers in $MgAl_2O_4$ spinels. Phys. Rev. B 44, 7256. https://doi.org/10.1103/PhysRevB.44.7256.
Känzig, W., Cohen, M.H., 1959. Paramagnetic resonance of oxygen in alkali halides. Phys. Rev. Lett. 3, 509–510. https://doi.org/10.1103/PhysRevLett.3.509.
Khamis, F., Arafah, D.E., 2021. Dead Sea salt as a thermoluminescent phosphor for beta irradiation dosimetry. Appl. Phys. A 127, 539. https://doi.org/10.1007/s00339-021-04463-3.
Khazal, K.A.R., Abul-Hail, R.Ch, 2010. Study of the possibility of using food salt as a gamma ray dosimeter. Nucl. Instrum. Methods B 624, 708–715. https://doi.org/10.1016/j.nima.2010.08.017.
Kitis, G., Gomez-Ros, J.M., Tuyn, W.N., 1998. Thermoluminescence glow-curve deconvolution functions for first, second and general orders of kinetics. J. Phys. D Appl. Phys. 31, 2636–2641. https://doi.org/10.1088/0022-3727/31/19/037.
Kittel, C., 1976. Introduction to Solid State Physics, fifth ed. John Wiley and Sons. Inc., New York.
McKeever, S.W.S., 1985. Thermoluminescence of Solids. Cambridge University Press, Cambridge.
Mehrabi, M., Zahedifar, M., Saeidi-Sogh, Z., Ramazani-Moghaddam-Arani, A., Sadeghi, E., Harooni, S., 2017. Thermoluminescence and photoluminescence properties of NaCl:Mn, NaCL:Cu nano-particles produced using co-precipitation and sono-chemistry methods. Nucl. Instrum. Methods A 846, 87–93. https://doi.org/10.1016/j.nima.2016.10.001.
Pagonis, V., Maniatis, Y., Michael, C., Bassiakos, Y., 1997. Spurious and regenerated thermoluminescence in calcite powder samples. Radiat. Meas. 27, 37–42. https://doi.org/10.1016/S1350-4487(96)00151-5.
Rodriguez-Lazcano, Y., Correcher, V., Garcia-Guinea, J., 2012. Luminescence emission of natural NaCl. Radiat. Phys. Chem. 81, 126–130. https://doi.org/10.1016/j.radphyschem.2011.07.012.
Roman-Lopez, J., López, Y.I.P., Cruz-Zaragoza, E., Marcazzó, J., 2018. Optically stimulated luminescence of natural NaCl mineral from Dead Sea exposed to gamma radiation. Appl. Radiat. Isot. 138, 60–64. https://doi.org/10.1016/j.apradiso.2017.05.001.
Spooner, N.A., Smith, B.W., Creighton, D.F., Questiaux, D., Hunter, P.G., 2012. Luminescence from NaCl for application to retrospective dosimetry. Radiat. Meas. 47, 883–889. https://doi.org/10.1016/j.radmeas.2012.05.005.
Spooner, N.A., Smith, B.W., Williams, O.M., Creighton, D.F., McCulloch, I., Hunter, P.G., Questiaux, D.G., Prescott, J.R., 2011. Analysis of luminescence from common salt (NaCl) for application to retrospective dosimetry. Radiat. Meas. 46, 1856–1861.
Tench, A.J., Nelson, R.L., 1967. Electron spin resonance of F centres in irradiated 43CaO and other alkaline earth oxides. Proc. Phys. Soc. 92, 1055. https://doi.org/10.1088/0370-1328/92/4/328.
Wahib, N.B., Sani, S.F.A., Ramli, A., Ismail, S.S., Jabar, M.H.A., Khandaker, M.U., Daar, E., Almugren, K.S., Alkallas, F.H., Bradley, D.A., 2020. Natural dead sea salt and retrospective dosimetry. Radiat. Environ. Biophys. 59, 523–537. https://doi.org/10.1007/s00411-020-00846-x.
Weast, R.C., 1971. CRC Handbook of Chemistry and Physics. In: Weast, R.C. (Ed.), 52nd edition. The Chemical Rubber Co., Cleveland.
Wertz, J.E., Auzins, P., Weeks, R.A., Silsbee, R.H., 1957. Centers in magnesium oxide; confirmation of the spin of magnesium-25. Phys. Rev. 107, 1535–1537. https://doi.org/10.1103/PhysRev.107.1535.